Dipeptidase-2 is a prognostic marker in lung adenocarcinoma that is correlated with its sensitivity to cisplatin

YUANYI WANG[1*], TING ZHANG[1,2*], HONGFEI DU[2*], MIN YANG[1,2], GUANGSU XIE[3], TENG LIU[1,2], SHIHUA DENG[1,2], WEI YUAN[1], SHUANG HE[1], DONGMING WU[1,2] and YING XU[1,2]

[1]College of Laboratory Medicine, Chengdu Medical College; [2]Clinical Laboratory, The First Affiliated Hospital of Chengdu Medical College; [3]Clinical Laboratory, Xindu District People's Hospital of Chengdu, Chengdu, Sichuan 610500, P.R. China

Received February 17, 2023; Accepted June 1, 2023

DOI: 10.3892/or.2023.8598

Abstract. Lung cancer accounts for the highest percentage of cancer morbidity and mortality worldwide, and lung adenocarcinoma (LUAD) is the most prevalent subtype. Although numerous therapies have been developed for lung cancer, patient prognosis is limited by tumor metastasis and more effective treatment targets are urgently required. In the present study, gene expression profiles were extracted from the Gene Expression Omnibus database and mRNA expression data were downloaded from The Cancer Genome Atlas database. In addition, TIMER 2.0 database was used to analyze the expression of genes in normal and multiple tumor tissues. Protein expression was confirmed using the Human Protein Atlas database and LUAD cell lines, sphere formation assay, western blotting, and a xenograft mouse model were used to confirm the bioinformatics analysis. Dipeptidase-2 (DPEP2) expression was significantly decreased in LUAD and was negatively associated with prognosis. DPEP2 overexpression substantially inhibited epithelial-mesenchymal transition (EMT) as well as LUAD cell metastasis, and limited the expression of the cancer stem cell transformation markers, CD44 and CD133. In addition, DPEP2 improved LUAD sensitivity to cisplatin by inhibiting EMT; this was verified *in vitro* and *in vivo*. These data indicated that DPEP2 upregulates E-cadherin, thereby regulating cell migration, cancer stem cell transformation, and cisplatin resistance, ultimately affecting the survival of patients with LUAD. Overall, the findings of the present suggest that DPEP2 is important in the development of LUAD and can be used both as a prognostic marker and a target for future therapeutic research.

Correspondence to: Professor Dongming Wu or Professor Ying Xu, Clinical Laboratory, The First Affiliated Hospital of Chengdu Medical College, 278 Baoguang Avenue, Xindu, Chengdu, Sichuan 610500, P.R. China
E-mail: harvey1989@126.com
E-mail: yingxu825@126.com

*Contributed equally

Abbreviations: CCK-8, Cell Counting Kit-8; DPEP2, dipeptidase-2; DPEP, dipeptidase family; EMT, epithelial-mesenchymal transition; FBS, fetal bovine serum; GEO, Gene Expression Omnibus; LTD4, leukotriene D4; LTE4, leukotriene E4; HPA, Human Protein Atlas; IF, immunofluorescence; IHC, immunohistochemistry; LUAD, lung adenocarcinoma; NSCLC, non-small cell lung cancer; OS, overall survival; ROC, receiver operating characteristic; RT-qPCR, reverse transcription-quantitative polymerase chain reaction; TCGA, The Cancer Genome Atlas; PD, progressive disease; SD, stable disease; PR, partial response; CR, complete response; IQR, interquartile range

Key words: DPEP2, biomarker, lung adenocarcinoma, cisplatin, EMT

Introduction

Lung cancer remains one of the malignancies with the highest incidence worldwide and a major cause of cancer-related deaths (1). Lung adenocarcinoma (LUAD) is the most prevalent histological subtype of non-small cell lung cancer (NSCLC), accounting for 40-55% of the cases (2,3). Although great progress has been made in the diagnosis and treatment of lung cancer, ~90% of lung cancer-related deaths are caused by metastasis (4). Currently, platinum compounds including cisplatin are first-line chemotherapy drugs for the majority of metastatic LUAD cases (5). However, LUAD can become resistant to treatment with additional cisplatin treatment cycles. Therefore, it is imperative to identify targets that improve LUAD sensitivity to chemotherapy.

One mechanism by which tumors metastasize is epithelial-mesenchymal transition (EMT). During this process, epithelial cells gain characteristics of mesenchymal cells; this process is associated with primary tumor formation, metastasis, and drug resistance (6). When cells undergo EMT, they lose cell polarity and the need for cell-cell adhesion for continued survival. In addition, mesenchymal markers, including N-cadherin, vimentin and α-smooth muscle actin, are upregulated, whereas epithelial markers, including E-cadherin, are downregulated; these post-EMT cells acquire migratory and invasive capabilities typical of mesenchymal cells (7,8). Because these changes enable tumor metastasis,

EMT regulators should be monitored in LUAD. For example, CD73, ELK1, and VPS33BD have been shown to promote LUAD progression by regulating EMT (9-11). Cancer cells that undergo EMT invade, metastasize, and exhibit cancer stem cell-like properties, conferring resistance to conventional and targeted therapies (12). In addition, mesenchymal-epithelial transition, the reverse process of EMT, plays a vital role in stem cell differentiation and dedifferentiation (13). Although numerous EMT regulators have been identified, other proteins or enzymes may contribute to this transformation.

Dipeptidase-2 (DPEP2), a member of the membrane-binding dipeptidase family (DPEP), is an extracellular enzyme fixed on the plasma membrane by glycosyl phosphatidylinositol and highly expressed in the lung, heart, and testis (14). The DPEP family is responsible for hydrolyzing dipeptides. For example, DPEP1 and DPEP2 can convert leukotriene D4 (LTD4) as a substrate to leukotriene E4 (LTE4), reducing or eliminating leukotriene activity (14-16). A previous study demonstrated that the expression of E-cadherin is increased by DPEP1 by inhibiting the LTD4 signaling pathway through the conversion of LTD4 to LTE4 (17). In addition, DPEP1 and DPEP3 have the ability to cleave cystinyl-*bis*-glycine to cysteine and glycine (14,15,18). Another related study suggested that DPEP1 is upregulated by dexamethasone in a glucocorticoid receptor-dependent manner to hydrolyze glutathione, thereby increasing dexamethasone sensitivity to ferroptosis (19). Notably, DPEP1 is the only enzyme known, to date, that is capable of hydrolyzing β-lactam substrates (14,18). However, the effects of members of the DPEP family, which hydrolyze substrates, remain to be fully elucidated and require further investigation.

A previous study indicated that macrophage DPEP2 can alleviate coxsackievirus B3-induced myocarditis by acting as a regulator of the NF-κB inflammatory signaling pathway (20). Recent studies have revealed that DPEP2 can be used as one of the risk-scoring factors of fatty acid metabolism genes in LUAD (21) and DPEP2 may constitute an immune indicator of LUAD (22). In addition, other DPEP family members have also been identified to be highly expressed in cancers. For instance, DPEP3 is associated with tumor-initiating cells in epithelial ovarian carcinoma (23). In addition, studies have shown that DPEP3 co-locates and forms a physical complex with TEX101 on the surface of murine testicular germ cells, which may be related to male infertility (24,25). Notably, DPEP1 exhibited the greatest degree of overexpression in colorectal cancer and knockdown of DPEP1 significantly increased cell apoptosis and attenuated cell proliferation as well as invasion (26,27). Similar studies have shown that DPEP1 is a biologically-related gene in pancreatic ductal adenocarcinoma with prognostic and therapeutic significance and overexpression of DPEP1 suppressed tumor cell invasiveness and increased sensitivity to chemotherapeutic agent gemcitabine (28). Furthermore, DPEP1 has been revealed to be highly expressed in hepatoblastoma and promoted the progression of hepatoblastoma via activating the phosphatidylinositol-3-kinase/Akt/mammalian target of rapamycin signaling (29). However, the expression, functions and mechanisms of DPEP2 in cancer, particularly in LUAD, remain poorly understood.

Therefore, in the present study the role of DPEP2 in LUAD was explored. DPEP2 expression in LUAD samples was analyzed with the use of public databases. The analysis included the gene, mRNA, and protein levels, and assessed the prognostic capabilities of DPEP2. Furthermore, the effects of DPEP2 in LUAD were investigated, both *in vitro* and *in vivo*, for the identification of targets which are able to disrupt EMT and metastasis. The present study highlighted the key role of DPEP2 in LUAD metastasis, and supports the clinical monitoring of this marker for assessment of prognosis.

Materials and methods

Patient datasets. As previously described (30), the gene expression profile GSE31210 (including 226 LUAD samples and 20 adjacent non-tumor samples) was downloaded from the Gene Expression Omnibus (GEO) database (https://www.ncbi.nlm.nih.gov/) for analysis (31,32). The inclusion criteria were as follows: i) The dataset only included LUAD tissue; ii) only included patients with LUAD; iii) was derived from human samples; iv) included a large number of patients between the ages of 30 and 70, as required by the study design; v) inclusion of stage I and II patients with LUAD, with ≥50 patient samples per stage; and vi) used high-throughput gene chips or sequencing technology. The exclusion criteria were as follows: i) The dataset contained a large number of missing or abnormal values; ii) the number of samples in each pathological stage of LUAD was limited in the dataset.

Furthermore, mRNA expression data, matched genome and clinical information (including 535 LUAD samples and 59 adjacent non-tumor samples) were downloaded from The Cancer Genome Atlas (TCGA) database (http://cancergenome.nih.gov/) for further analytical verification. The inclusion criteria were as follows: i) The data of the samples were sourced from TCGA database; ii) consisted of LUAD samples; iii) the inclusion of mRNA expression data, matched genome data, and clinical information; iv) complete clinical information including pathological stage, differentiation degree, survival time, sex, age, etc.; v) the mRNA expression data was assessed using RNA-seq technology and included high-quality expression data (such as RPKM, FPKM, etc.); and vi) the genomic data were matched and the gene annotation information was the latest. The exclusion criteria were as follows: i) The data of samples were limited; ii) the quality of the expression data was poor, including lowly-expressed genes, missing values, etc.; and iii) the genomic data did not match, or gene annotation information was incomplete.

The gene amplification and mutation status of DPEP2 was obtained using cBioPortal for Cancer Genomics (http://www.cbioportal.org/). Briefly, the module of 'Query-Lung-Lung Adenocarcinoma (TCGA, Nature 2014)' was selected on the homepage, 'Query By Gene' was clicked, 'DPEP2' was entered, and 'Submit Query' was then clicked to submit the analysis. The Human Protein Atlas (HPA) database (http://www.proteinatlas.org/) was used to verify the expression of DPEP2 in LUAD. Briefly, 'DPEP2' was entered in the homepage for query, 'TISSUE' and then 'LUNG' was selected to obtain the normal group images; in addition, 'PATHOLOGY' and then 'CANCER-LUNG CANCER' were selected to obtain images.

Establishment and evaluation of LUAD survival prediction. Cox regression analysis was used to screen independent

clinicopathological prognostic factors and construct a contingency table to assess the 1-, 3-, and 5-year overall survival (OS) probability in patients with LUAD. Its accuracy was verified by comparing its predicted probability with the actual probability observed in the correction curve. Receiver operating characteristic (ROC) curve analysis was used to compare the predicted accuracy of the combined model line chart and the clinicopathological prognostic factor line chart.

TIMER2.0 database analysis. TIMER2.0 database (http://timer.cistrome.org/) was used to analyze the expression levels of genes in normal and multiple tumor tissues extracted from TCGA. Briefly, the module of 'Cancer Exploration' on the homepage was selected, and then 'DPEP2' and 'Submit' were selected in order to perform the analysis.

Cell culture. A549 (cat. no. CRL-7909; NSCLC cell line; was initiated by explant culture of lung carcinomatous tissue from a 58-year-old Caucasian male; a hypotriploid human cell line with the modal chromosome number of 66, occurring in 24% of cells; mutations: KRAS, STK11, TP53) and H1650 (cat. no. CRL-5883; human NSCLC cell line; this was a cell line exhibiting epithelial morphology that was isolated in 1987 from the lung tissue of a 27-year-old, male smoker with stage 3B, bronchoalveolar carcinoma; mutations: EGFR, TP53) cell lines were obtained from the American Type Culture Collection. BEAS-2B (cat. no. F26092; Chengdu Feiouer Biotechnology Co., Ltd.; a human lung bronchial epithelial cell line; this was isolated from pathological sections of normal bronchial epithelium from a non-cancerous individual) and H1299 (cat. no. F26035; Chengdu Feiouer Biotechnology Co., Ltd.; human NSCLC cell line; this was isolated from the lung of a Caucasian, 43-year-old, male patient with carcinoma; gene deletion: TP53; mutation: NRAS) cell lines were obtained from Feiouer Biological Technology Co. The tissue origins of A549, H1650 and H1299 were from patients with lung cancer, and the tissue origin of BEAS-2B was from a non-lung cancer patient. All cells were authenticated using short tandem repeat (STR) DNA profiling analysis. The STR appraisal reports were issued by Procell Life Science & Technology Co., Ltd. and Chengdu Feiouer Biotechnology Co., Ltd. The cells were cultured in RPMI-1640 medium (Invitrogen; Thermo Fisher Scientific, Inc.) supplemented with 10% fetal bovine serum (FBS; Procell Life Science & Technology Co., Ltd.) and 5 mg/ml penicillin/streptomycin (Invitrogen; Thermo Fisher Scientific, Inc.) and were maintained in a humidified incubator with 5% CO_2 at 37˚C.

Cell transfection. DPEP2-overexpressing lentivirus (PGMLV-CMV-H_DPEP2-3xFlag-PGK-Puro; transcript no. NM_022355.4; https://www.ncbi.nlm.nih.gov/nuccore/NM_022355.4/) and empty lentivirus (GM-18844: PGMLV-CMV-MCS-3xFlag-PGK-Puro) were constructed and packaged by Genomeditech (Shanghai) Co., Ltd. (https://www.genomeditech.com/). For this experiment, the 2nd generation system, and the interim cell line, 293T cells (Genomeditech (Shanghai) Co., Ltd.), were used. A549 and H1650 cell lines, were divided into an empty vector group (Vector) and a pGMLV-CMV-DPEP2-overexpression group (DPEP2). Firstly, $2x10^5$ cells/well were seeded in six-well plates, and when the cell density reached ~70%, fresh medium was replaced. Subsequently, 10 μl of lentivirus liquid (virus titer, $1x10^8$ TU/ml; multiplicity of infection: 10) was added, and polybrene [Genomeditech (Shanghai) Co., Ltd.] was added at the same time to increase infection efficiency so that the final concentration reached 8 μg/ml. After 24 h of transfection at 37˚C, the medium was changed, and the cells successfully transfected with the virus were screened and maintained with a final concentration of 1 μg/ml of puromycin dihydrochloride (cat. no. ST551-10 mg; Beyotime Institute of Biotechnology). The survival state of the cells was observed every 24 h. After two days, the cells of the Vector and DPEP2 groups began to proliferate. After one week, transfection efficiencies were evaluated using reverse transcription-quantitative PCR (RT-qPCR) and western blotting.

Total RNA extraction and RT-qPCR. Total RNA was extracted from the cells on ice according to the instructions of the Total RNA Extraction Kit (Beijing Solarbio Science & Technology Co., Ltd.). RNA samples were reverse transcribed using the iScript cDNA Synthesis Kit (Bio-Rad Laboratories, Inc.) according to the manufacturer's instructions. The cDNAs were then added to the reaction with the indicated primers using SYBR Green Supermix (Bio-Rad Laboratories, Inc.) on ice according to the manufacturer's instructions and amplified using RT-qPCR, performed at 95˚C for 2 min, followed by 40 cycles of amplification at 95˚C for 10 sec, 62˚C for 30 sec and 72˚C for 30 sec using a CFX96 Real-Time PCR Detection System (Bio-Rad Laboratories, Inc.). β-actin was used as an endogenous control. Relative gene expression levels were calculated by normalizing the transcript levels to the housekeeping gene using the comparative threshold cycle $2^{-\Delta\Delta Cq}$ method (33). The primers used were as follows: DPEP2 forward, 5'-ATC ATGCCCAGGCGGTTCATTTC-3' and reverse, 5'-GGCGTC CACTCCTTCTACAACAAC-3'; β-actin forward, 5'-GGG CCGGACTCGTCATAC-3' and reverse, 5'-CCTGGCACC CAGCACAAT-3'.

Western blotting. Cells were lysed with radioimmunoprecipitation assay buffer containing the protease inhibitor phenylmethylsulfonyl fluoride (Beyotime Institute of Biotechnology). The protein concentration was determined using a BCA Protein Determination Kit (Beyotime Institute of Biotechnology) according to the manufacturer's instructions. Protein samples (30 μg) were separated on 10% gels using sodium dodecyl sulfate-polyacrylamide gel electrophoresis and transferred to 0.2-μm polyvinylidene fluoride membranes (Immobilon-P PVDF; EMD Millipore). The membranes were blocked using Tris-buffered saline containing 0.1% Tween-20 and 5% skim milk for 1 h at 25˚C. The membranes were incubated with the primary antibodies, including anti-DPEP2 (1:1,000; cat. no. 16466-1-AP), anti-E-cadherin (1:2,000; cat. no. 60335-1-Ig), anti-N-cadherin (1:2,000; cat. no. 66219-1-Ig), anti-vimentin (1:20,000; cat. no. 60330-1-Ig), anti-α-SMA (1:1,000; cat. no. 14395-1-AP), anti-CD44 (1:2,000; cat. no. 15675-1-AP), anti-CD133 (1:2,000; cat. no. 18470-1-AP), anti-GADPH (1:50,000; cat. no. 60004-1-Ig; all from Proteintech Group, Inc.), overnight at 4˚C. After washing three times with Tris-buffered saline with 0.1% Tween-20, the membranes were incubated

with corresponding horseradish peroxidase-conjugated secondary antibodies [cat. no. SA00001-1 (mouse); SA00001-2 (rabbit); 1:4,000; both from Proteintech Group, Inc.] for 1.5 h at 25˚C. The bands were visualized in conjunction with ECL Detection Reagents (EMD Millipore) using the Quantity One 5.2 Software System (Bio-Rad Laboratories, Inc.).

Wound-healing assays. A549 and H1650 cells ($5x10^5$; treatment with or without DPEP2 overexpression) cultured in serum-free medium for 24 h were seeded on a six-well plate and allowed to reach nearly 100% confluence. The cell monolayer was scratched with a 200-μl sterile pipette tip to create an artificial wound, and the cell debris was removed by repeated washes with PBS. Subsequently, the cells were cultured in fresh serum-free medium and kept in a humidified incubator with 5% CO_2 at 37˚C. At 0 and 12 h, the wound-healing process was captured at a magnification of x10 under a fluorescence microscope (Eclipse Ti Series; Nikon Corporation).

Cell migration and invasion assay. As previously described (34), $1x10^5$ A549 and H1650 cells (treatment with or without DPEP2 overexpression) cultured in serum-free medium for 24 h were seeded into the upper lumen of an 8-μm pore size Transwell insert (Corning, Inc.) for the migration assay, and another set of $1x10^5$ cells were seeded into the upper lumen of pre-coated Matrigel (at 37˚C for 1 h) (BD Biosciences) for the invasion assay. Medium containing 10% FBS was added to the lower lumen as an attractant. For both experiments, cells were incubated for 24 h at 37˚C and 5% CO_2. For the migration experiment, the Transwell container was removed and washed with sterile PBS. For both experiments the cells were then fixed with methanol for 20 min and stained with 0.1% crystal violet for 20 min at 25˚C. The cells that had not migrated were removed with cotton swabs and images were captured at a magnification of x20 under a fluorescence microscope, and were subsequently counted (XI71; Olympus Corporation).

Sphere formation assay. A549 and H1650 cells (treatment with or without DPEP2 overexpression) were digested with 0.25% Trypsin-EDTA (Invitrogen; Thermo Fisher Scientific, Inc.), centrifuged with a low centrifugation speed (141 x g for 3 min at 25˚C; model no. JW-1016; Anhui Jiawen Instrument Equipment Co., Ltd.), and washed thrice with PBS. The cells were resuspended in Dulbecco's modified Eagle's medium/F12 medium (Invitrogen; Thermo Fisher Scientific, Inc.) supplemented with 20 ng/ml Epidermal Growth Factor (MedChemExpress), 20 ng/ml Basic Fibroblast Growth Factor (MedChemExpress), and 1X B-27 supplement (Invitrogen; Thermo Fisher Scientific, Inc.). Cells were incubated at a density of $5x10^3$ cells/well in a six-well ultra-low adhesion plate for 7-10 days at 37˚C with 5% CO_2. Representative tumor spheres were captured at a magnification of x20 and quantified under a fluorescence microscope (Eclipse Ti Series; Nikon Corporation).

Immunofluorescence (IF). The prepared cell slides were carefully washed with PBS, fixed with 4% paraformaldehyde for 15 min at 25˚C, washed repeatedly with PBS, and blocked with PBS containing 10% normal goat serum (cat. no. C0265; Beyotime Institute of Biotechnology) for 1 h at 25˚C. The slides were incubated with primary antibodies, including anti-E-cadherin (1:200; cat. no. 60335-1-Ig), anti-N-cadherin (1:50; cat. no. 66219-1-Ig), anti-vimentin (1:50; cat. no. 60330-1-Ig), anti-α-SMA (1:800; cat. no. 14395-1-AP), anti-CD44 (1:50; cat. no. 15675-1-AP), and anti-CD133 (1:50; cat. no. 18470-1-AP; all from Proteintech Group, Inc.), overnight at 4˚C. After multiple rinses with PBS, the slides were incubated with Cy3 (red)-conjugated secondary antibodies [1:300; cat. no. A0516 (goat anti-rabbit); A0521 (goat anti-mouse); Beyotime Institute of Biotechnology] at room temperature for 2 h in the dark. The samples were washed three times with PBS and stained with DAPI (1:4,000; cat. no. C1002; Beyotime Biotechnology) for 5 min at 25˚C before imaging. Random images were captured at a magnification of x40 with an inverted fluorescence microscope (IX71; Olympus Corporation).

Cell viability assays. Cell viability was determined using a Cell Counting Kit-8 (CCK-8) and colony formation assays. Briefly, for the colony formation assay, the cells were cultured in a six-well plate at a ratio of 600 cells/well with varying concentrations of cisplatin (0, 2, 4, or 8 μg/ml; Jiangsu Hansoh Pharmaceutical Group Co., Ltd.). The medium containing varying concentrations of cisplatin was changed every 3 days, and cells were cultured for 14 days at 37˚C. After the colonies were washed with PBS, they were fixed with methanol for 15 min at 25˚C and stained with 0.1% crystal violet for 20 min at 25˚C. Colonies were defined as >50 ells and were counted manually. The CCK-8 assay was performed according to the instructions of the Enhanced Cell Counting Kit-8 (Beyotime Institute of Biotechnology). A549 and H1650 cells ($5x10^3$; treatment with or without DPEP2 overexpression) were seeded into 96-well cell culture plates followed by treatment with cisplatin (0, 2, 4 or 8 μg/ml) at 37˚C for 24 h. The medium in each well was then replaced with 100 μl fresh medium with 10% CCK-8 and the cells were incubated at 37˚C for an additional 1 h. The absorbance was measured at 450 nm.

Flow cytometry. A549 and H1650 cells (treatment with or without DPEP2 overexpression) with a density of 70%, treated with or without 2 μg/ml cisplatin for 24 h at 37˚C, were digested with 0.25% Trypsin (Invitrogen; Thermo Fisher Scientific, Inc.), washed twice with PBS and collected. Cells were stained for 15 min in the dark at 25˚C using the Annexin V-PE/7-AAD Apoptosis Detection Kit (Nanjing KeyGen Biotech Co., Ltd.), according to the manufacturer's instructions. Cells were analyzed using flow cytometry (FACSCalibur; Becton, Dickinson and Company).

Immunohistochemistry (IHC). IHC was performed using a Universal two-step detection kit (mouse/rabbit enhanced polymer detection system; cat. no. PV9000; ZSGB-BIO; OriGene Technologies, Inc.). The prepared 5-μm paraffin sections were dewaxed, dehydrated in a liquid gradient, and washed several times with PBS. Sections were then boiled in a pH 6.0 citric acid buffer for target antigen retrieval. Subsequently, endogenous peroxidase was blocked according to the manufacturer's instructions. The sections were incubated with the primary antibodies, including

anti-DPEP2 (1:200; cat. no. 16466-1-AP), anti-E-cadherin (1:1,000; cat. no. 60335-1-Ig), anti-N-cadherin (1:8,000; cat. no. 66219-1-Ig), anti-vimentin (1:4,000; cat. no. 60330-1-Ig), anti-α-SMA (1:2,000; cat. no. 14395-1-AP), anti-CD44 (1:500; cat. no. 15675-1-AP), anti-CD133 (1:4,000; cat. no. 18470-1-AP), anti-Ki67 (1:2,000; cat. no. 27309-1-AP; all from Proteintech Group, Inc.), at 4˚C overnight. After multiple rinses using PBS, the sections and reaction enhancement solution were incubated at 25˚C for 20 min. After multiple rinses using PBS, the immune complexes were incubated with the corresponding enzyme-conjugated secondary antibodies (cat. no. PV9000; ZSGB-BIO; OriGene Technologies, Inc.) for 30 min at 37˚C.

Finally, the sections were dyed with a 3,3'-diaminobenzene (DAB) Chromogenic kit (cat. no. ZLI-9019; ZSGB-BIO; OriGene Technologies, Inc.). Briefly, DAB was used as the chromogen to stain the reaction products for 3 min at room temperature for visualization. The sections were then counterstained with hematoxylin (Beyotime Institute of Biotechnology) at room temperature for 1 min. Random images were obatined at a magnification of x20 using a fluorescence microscope (IX71; Olympus Corporation).

Nude mouse subcutaneous tumor model. A total of 16, five-week-old nude female BALB/c mice with a weight of 18-20 g (GemPharmatech Co. Ltd.) were used for *in vivo* experiments. All nude mice were kept at an auto-controlled room (24±2˚C; 50±10%, relative humidity) with 12-h light/dark cycle. Nude mice were acclimatized for least 7 days before experiments, and allowed free access to food and water. All nude mice were randomly divided into 4 groups with 4 mice per group (vector; DPEP2; vector + cisplatin; DPEP2 + cisplatin). Vector or DPEP2-overexpressing A549 cells ($2x10^6$) were resuspended in 100 μl of serum-free RPMI-1640 medium, and subcutaneously injected into the left armpit of each nude mouse in each group. Subsequently, seven days after A549 cell implantation, each group was intraperitoneally injected with either 100 μl PBS or cisplatin (20 mg/m^2/mouse/week). The tumor growth in each group (n=4/group) was measured with Vernier calipers every seven days. The formula, $V=(a \times b^2)/2$ was used to calculate the tumor volume, where a and b are the maximum and minimum diameters, respectively, in millimeters. On day 28 after the cell injection, all tumors images were captured, and the nude mice were then euthanized by intraperitoneal injection of 100 mg/kg sodium pentobarbital until cardiac arrest and spontaneous respiratory arrest. The tumors were weighed and their images were captured immediately after dissection.

Statistical analysis. The R software package 'limma' (version 3.40.6; R Foundation for Statistical Computing) was used to perform gene expression differential analysis. DPEP2 expression data were divided using the median method, and duplicate samples were excluded. The Wilcoxon signed-rank test and logistic regression was used to assess the correlation between the clinicopathological characteristics of LUAD and DPEP2 expression. Univariate and multivariate Cox analyses were used to identify potential prognostic factors. Kaplan-Meier plotter and log-rank testing were used to evaluate the OS. Each *in vitro* experiment was independently performed at least three times. Data were analyzed using GraphPad Prism 8.0 statistical program (GraphPad Software, Inc.). Results are presented as the mean ± standard deviation unless otherwise stated. The Shapiro-Wilk normality test was used to determine if the data followed normal distribution. If the data followed normal distribution, the results were presented as the mean ± standard, and the two-tailed Student's independent samples t-test or one-way ANOVA was used to analyze the significance of the differences between two groups or multiple groups. The post hoc tests used following ANOVA were Dunnett's t-test to compare one group with the other groups, or Newman-Keuls to determined which specific pairs of means were different. When the normality assumption was violated, Kruskal-Wallis test was used to determine statistically significant differences between three or more independent groups, and Bonferroni correction was applied for the post hoc multiple comparisons. For all hypotheses tests, a $P<0.05$ was considered to indicate a statistically significant difference.

Results

Expression of DPEP2 is low in LUAD. Differential expression analysis of RNA sequencing data of LUAD samples was performed in GSE31210 to identify genes that exhibited consistent expression changes with LUAD progression. *DPEP2* was among the genes that were notably negatively associated with LUAD progression (Fig. 1A). *DPEP2* mRNA levels in different tumors and corresponding normal tissues were confirmed using the TIMER2.0 database. *DPEP2* expression was significantly lower in LUAD than in normal tissues (Fig. 1B). To assess the mutation level of *DPEP2*, a cBioPortal map was used to analyze the OncoPrint map of *DPEP2* in patients with LUAD in TCGA dataset (Fig. 1C), which revealed that *DPEP2* had less than 2.2% missense mutations and gene amplifications.

DPEP2 mRNA expression levels were then assessed in patients with LUAD and adjacent tissues. As a result, *DPEP2* expression was identified to be significantly lower in patients with LUAD than in precancerous tissue ($P<0.01$; Fig. 1D). Similar results were obtained by comparing *DPEP2* expression levels in LUAD and paired precancerous tissues (Fig. 1E). In addition, DPEP2 transcription and protein expression levels were analyzed *in vitro*, and it was demonstrated that the levels in LUAD cells were significantly lower than that in a normal lung cell line ($P<0.001$; Fig. 1F and H). Based on the HPA database results, it was revealed that DPEP2 levels were lower in the tumors than in precancerous tissues (Fig. 1G). Therefore, these data indicated that DPEP2 was considerably downregulated in LUAD.

DPEP2 is an independent prognostic factor for the OS of patients with LUAD. The role of DPEP2 was investigated in patients with LUAD. The results revealed that low DPEP2 expression was associated with sex ($P<0.05$), age ($P<0.05$), smoking status ($P<0.01$), tumor (T) stage ($P<0.05$), node (N) stage ($P<0.05$), and clinical stage ($P<0.01$; Fig. 2A-F and Table I). These results indicated that patients with LUAD with low *DPEP2* expression progress to advanced disease faster than those with high *DPEP2* expression.

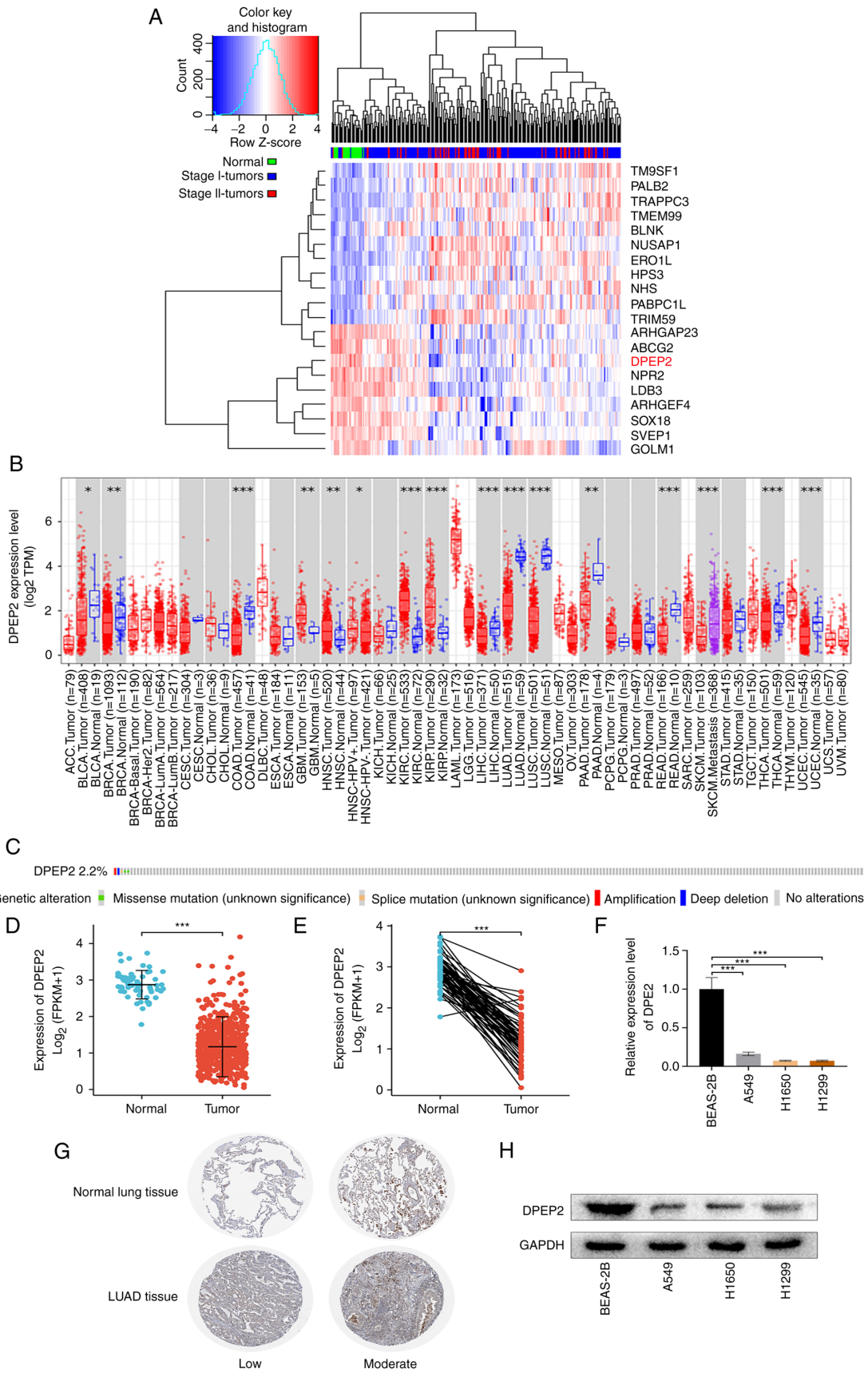

Figure 1. Expression levels of DPEP2 in generalized carcinoma and LUAD. (A) The heatmap of the top ten upregulated and downregulated genes with LUAD progression based on RNA sequencing data in Gene Expression Omnibus (GSE31210). (B) The expression level of DPEP2 in different tumors in TCGA was determined using TIMER2.0. (C) The cBioPortal OncoPrint map shows the distribution of DPEP2 genome changes in patients with LUAD. (D) Expression level of DPEP2 in normal tissues and tumor tissues. (E) Expression level of DPEP2 in normal tissues and the paired adjacent tumor tissues. (F) Transcriptional level of DPEP2 in the human lung bronchial epithelial cell line BEAS-2B and various LUAD cell lines (A549, H1650, and H1299). (G) Validation of the expression level of DPEP2 in LUAD using the Human Protein Atlas database (immunofluorescence). (H) The protein levels of DPEP2 were determined using western blotting in different LUAD cell lines. *P<0.05, **P<0.01 and ***P<0.001; two-tailed Student's t-test. DPEP2, dipeptidase-2; LUAD, lung adenocarcinoma.

Table I. Association between DPEP2 expression and the clinicopathological features of lung adenocarcinoma cases in The Cancer Genome Atlas.

Characteristics	Low expression of DPEP2 (n=256)	High expression of DPEP2 (n=257)	P-value
T stage, n (%)			0.015
T1	70 (13.7%)	98 (19.2%)	
T2	144 (28.2%)	132 (25.9%)	
T3	27 (5.3%)	20 (3.9%)	
T4	14 (2.7%)	5 (1%)	
N stage, n (%)			0.023
N0	152 (30.3%)	178 (35.5%)	
N1	52 (10.4%)	43 (8.6%)	
N2	47 (9.4%)	27 (5.4%)	
N3	1 (0.2%)	1 (0.2%)	
M stage, n (%)			0.500
M0	175 (47.4%)	169 (45.8%)	
M1	15 (4.1%)	10 (2.7%)	
Pathologic stage, n (%)			0.009
Stage I	119 (23.6%)	155 (30.7%)	
Stage II	64 (12.7%)	57 (11.3%)	
Stage III	53 (10.5%)	31 (6.1%)	
Stage IV	15 (3%)	11 (2.2%)	
Primary therapy outcome, n (%)			0.031
PD	43 (10.1%)	25 (5.9%)	
SD	19 (4.5%)	18 (4.2%)	
PR	4 (0.9%)	2 (0.5%)	
CR	141 (33.1%)	174 (40.8%)	
Residual tumor, n (%)			0.609
R0	178 (49.3%)	166 (46%)	
R1	7 (1.9%)	6 (1.7%)	
R2	1 (0.3%)	3 (0.8%)	
Age, n (%)			0.004
≤65	135 (27.3%)	103 (20.9%)	
>65	111 (22.5%)	145 (29.4%)	
Sex, n (%)			0.030
Female	125 (24.4%)	151 (29.4%)	
Male	131 (25.5%)	106 (20.7%)	
Number pack years smoked, n (%)			0.492
<40	87 (24.8%)	87 (24.8%)	
≥40	96 (27.4%)	81 (23.1%)	
Smoker, n (%)			0.014
No	27 (5.4%)	47 (9.4%)	
Yes	224 (44.9%)	201 (40.3%)	
OS event, n (%)			0.016
Alive	149 (29%)	177 (34.5%)	
Dead	107 (20.9%)	80 (15.6%)	
Age, median (IQR)	64 (58, 71)	68 (59, 73.25)	0.007

DPEP2, dipeptidase-2; PD, progressive disease; SD, stable disease; PR, partial response; CR, complete response; OS, overall survival; IQR, interquartile range.

In addition, treatment outcomes (P<0.01) and OS (P<0.001) were associated to low *DPEP2* expression (Fig. 2G and H). To further explore the association between the survival rate and clinicopathological features, univariate Cox regression

Table II. Univariate and multivariate Cox regression analysis of clinical features associated with overall survival of lung adenocarcinoma in The Cancer Genome Atlas.

		Univariate analysis		Multivariate analysis	
Characteristics	Total (N)	Hazard ratio (95% CI)	P-value	Hazard ratio (95% CI)	P-value
Age (≤65 vs. >65)	494	1.228 (0.915-1.649)	0.171		
Sex (female vs. male)	504	1.060 (0.792-1.418)	0.694		
T stage (T1/T2 vs. T3/T4)	501	2.364 (1.621-3.448)	<0.001	1.882 (0.900-3.939)	0.093
N stage (N0 vs. N1 and N2 and N3)	492	2.606 (1.939-3.503)	<0.001	1.593 (0.966-2.627)	0.068
M stage (M0 vs. M1)	360	2.111 (1.232-3.616)	0.007	1.502 (0.558-4.044)	0.420
Pathologic stage (stage I/stage II vs. stage III/stage IV)	496	2.624 (1.926-3.576)	<0.001	1.471 (0.725-2.983)	0.285
Primary therapy outcome (PR and CR vs. PD and SD)	419	2.786 (1.978-3.924)	<0.001	3.129 (1.883-5.200)	<0.001
Residual tumor (R0 vs. R1 and R2)	352	3.973 (2.217-7.120)	<0.001	3.373 (1.287-8.839)	0.013
Number pack years smoked (<40 vs. ≥40)	345	1.038 (0.723-1.490)	0.840		
DPEP2 (low vs. high)	504	0.643 (0.479-0.862)	0.003	0.955 (0.603-1.512)	0.843

TCGA, The Cancer Genome Atlas; CI, confidence interval; DPEP2, dipeptidase-2; PR, partial response; CR, complete response; PD, progressive disease; SD, stable disease.

analysis was conducted, and it was revealed that DPEP2 was significantly associated with OS (hazard ratio, 0.643; 95% confidence interval, 0.479-0.862; P=0.003) (Table II). Multivariate Cox regression analysis demonstrated that the primary therapeutic outcome and residual tumors were independent prognostic factors (Table II). Additionally, low *DPEP2* expression was associated with poor patient prognosis (hazard ratio, 0.63; 95% confidence interval, 0.47-0.84; P=0.002) (Fig. 2I). These results indicated that *DPEP2* was a prognostic factor for LUAD. To analyze the diagnostic value of *DPEP2* expression, a ROC curve was constructed and nomogram analysis of *DPEP2* expression data was performed. The area under the ROC curve was 0.976 (Fig. 2J). *DPEP2* expression levels were combined with clinical variables to construct a nomogram to predict patient survival at 1, 3, and 5 years. The predictive power of *DPEP2* expression was comparable to that of the T stage, which is the most common tumor staging system worldwide (Fig. 2K). These findings indicated that DPEP2 may serve as a prognostic biomarker in LUAD.

DPEP2 inhibits cell migration, invasion and EMT in LUAD. To determine the role of DPEP2 in the malignant progression of LUAD, stable A549 and H1650 cell lines overexpressing DPEP2 were constructed. Both RT-qPCR and western blotting revealed that DPEP2 mRNA and protein expression were considerably upregulated (Fig. 3A). The wound-healing assay revealed that DPEP2 overexpression inhibited the migratory abilities of cells (Fig. 3B). In Transwell assays, DPEP2 overexpression inhibited cell migration and invasion (Fig. 3C and D). Furthermore, western blotting and IF results revealed that DPEP2 overexpression increased E-cadherin levels and decreased N-cadherin, vimentin, and α-SMA levels (Fig. 3E and F). These data indicated that DPEP2 inhibited LUAD cell migration, invasion, and EMT.

DPEP2 enhances cell sensitivity to cisplatin by regulating stem cell transformation. Research has revealed that tumor cell EMT can lead to the same chemotherapy resistance as cancer stem cells (35). Therefore, it was hypothesized that DPEP2 may affect the chemotherapy response by regulating EMT. Consequently, the levels of DPEP2 and the lung cancer stem cell biomarkers, CD44 and CD133, were assessed using western blot and IF analyses. It was determined that DPEP2 overexpression significantly decreased CD44 and CD133 in two LUAD cell lines (P<0.001; Fig. 4A and B). In addition, DPEP2 overexpression significantly decreased sphere formation in A549 (P<0.01; Fig. 4C) and H1650 cells (P<0.001; Fig. 4C). These results indicated that DPEP2 overexpression inhibited cancer stem cell-like traits in LUAD.

The functional significance of DPEP2 expression in cisplatin resistance was further explored. Notably, colony formation and CCK-8 assays demonstrated that DPEP2 promoted cisplatin-induced A549 and H1650 cell death (Fig. 4D-F). Apoptosis assays revealed similar findings, wherein DPEP2-overexpressing A549 and H1650 cells had higher apoptosis rates and higher sensitivity to cisplatin (Fig. 4G).

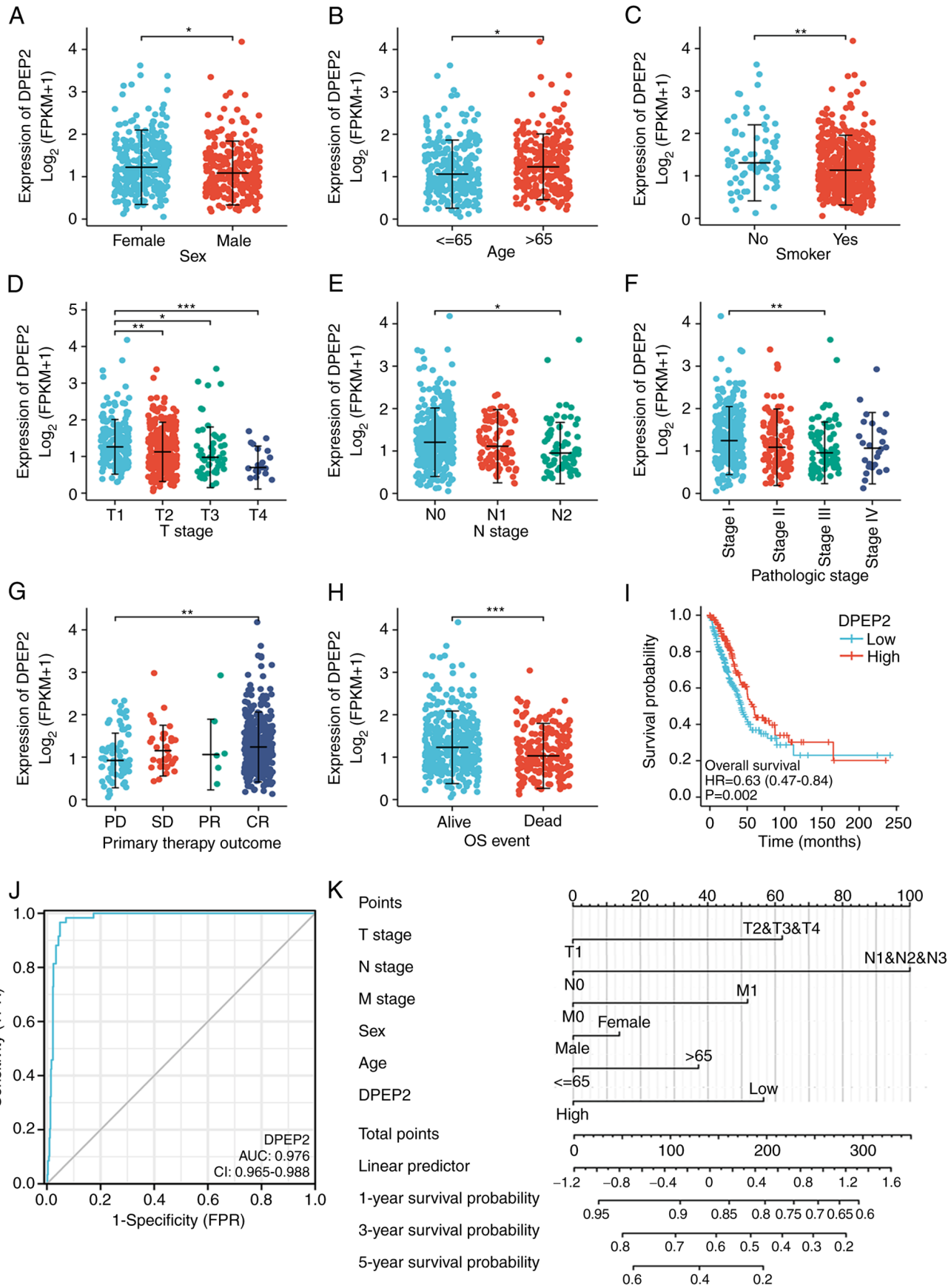

Figure 2. Association between DPEP2 expression and clinicopathological features and its prognostic and diagnostic value in LUAD. (A-H) The tumor tissues from patients with different clinical characteristics in TCGA. (A) Sex, (B) age, (C) smoking status, (D) T stage, (E) N stage, (F) pathologic stage, (G) primary treatment outcome and (H) OS; A-C and H: *P<0.05, **P<0.01 and ***P<0.001, two-tailed Student's *t*-test; and D-G: *P<0.05, **P<0.01 and ***P<0.001, one-way ANOVA with Bonferroni correction. (I) Kaplan-Meier analysis of the OS probability of patients with LUAD in TCGA. (J) Receiver operating characteristic curve analysis for DPEP2 expression in LUAD and adjacent tissues. (K) Nomogram survival prediction chart for predicting the 1-, 3-, and 5-year OS rates. DPEP2, dipeptidase-2; LUAD, lung adenocarcinoma; TCGA, The Cancer Genome Atlas; OS, overall survival.

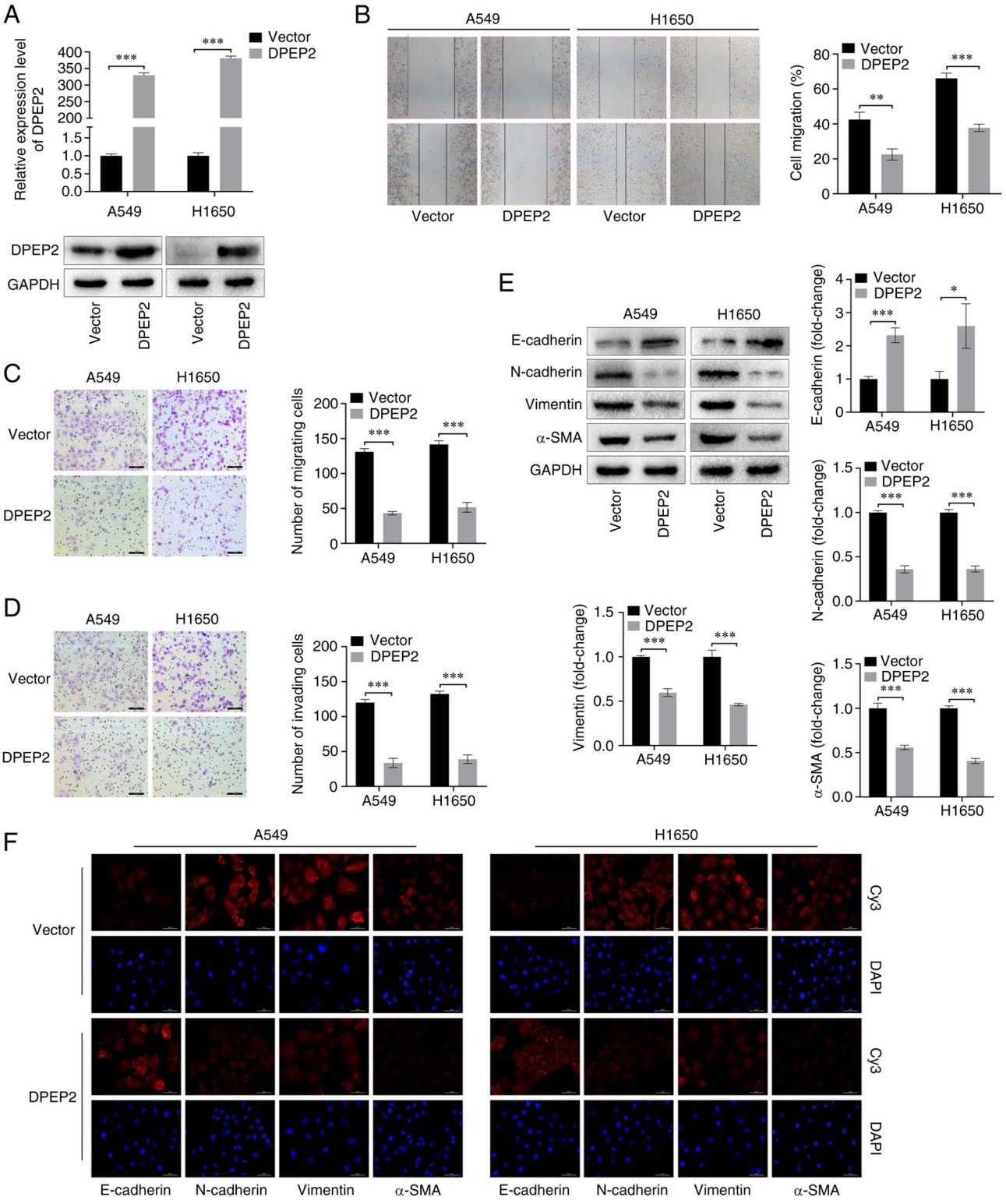

Figure 3. DPEP2 affects migration, invasion, and EMT of lung adenocarcinoma cells. (A) Expression of DPEP2 in empty vector control (Vector) and DPEP2-overexpressing cells (DPEP2) was detected using western blotting and reverse transcription-quantitative PCR assays. GAPDH served as a loading control. (B) Representative images and quantitative analysis of wound-healing assay of A549 and H1650 cells (scale bar, 200 μm). (C and D) Transwell representative images and analysis of (C) cell migration and (D) invasion (scale bar, 100 μm). (E and F) The EMT markers (E-cadherin, N-cadherin, vimentin, and α-SMA) were analyzed using western blot analysis and IF staining (scale bar, 50 μm). Histograms represent the mean ± standard deviation based on three independent experiments. *P<0.05, **P<0.01 and ***P<0.001, two-tailed Student's t-test. DPEP2, dipeptidase-2; EMT, epithelial-mesenchymal transition.

DPEP2 enhances the sensitivity of LUAD to cisplatin in vivo. To further investigate the effect of DPEP2 on cisplatin treatment, a nude mouse subcutaneous tumor model was established using A549 cells (Fig. 5A). It was demonstrated that DPEP2 overexpression significantly increased cisplatin efficacy compared with the control group, as revealed in the tumor chart (Fig. 5B and C). Similar results were obtained by dissection and weight comparisons (Fig. 5D and E). In subsequent

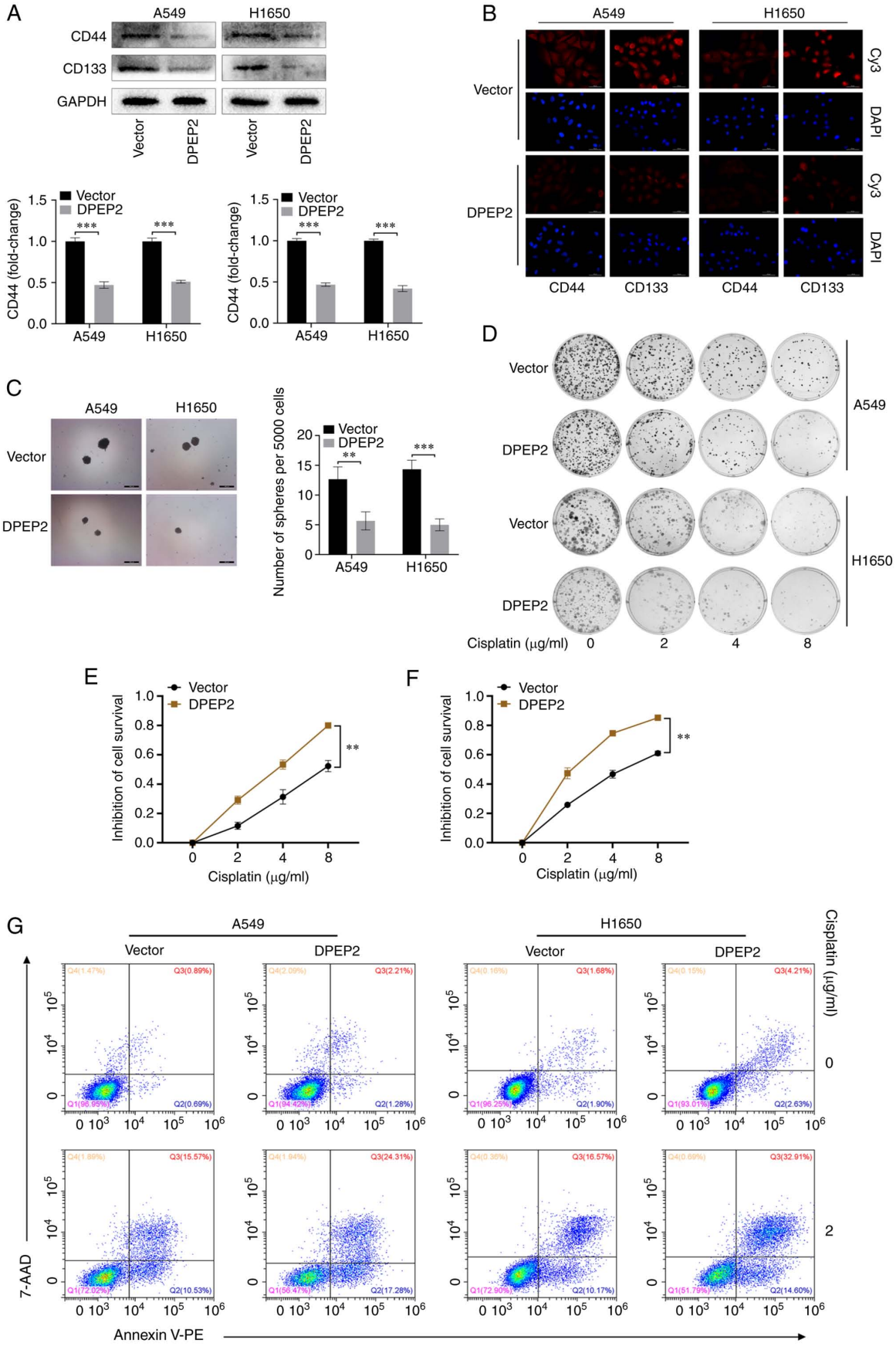

Figure 4. DPEP2 enhances lung adenocarcinoma cell sensitivity to cisplatin by regulating cancer stem cell transformation. (A and B) Expression of CD44 and CD133 was determined by western blotting and immunofluorescence staining (scale bar, 50 μm). (C) Representative images and analysis of sphere formation in A549 and H1650 cells (scale bar, 100 μm). (D) Representative images of colony formation assays of A549 and H1650 cells treated with various concentrations of cisplatin at 0, 2, 4 or 8 μg/ml. (E and F) Cell Counting Kit-8 assay was used to analyze the sensitivity of A549 and H1650 cells to various concentrations of cisplatin at 0, 2, 4 or 8 μg/ml. **P<0.01, two-way ANOVA with post hoc Dunnett's t-test. (G) Representative flow cytometric images of A549 and H1650 cells treated with 0 or 2 μg/ml cisplatin. **P<0.01 and ***P< 0.001, two-tailed Student's t-test. DPEP2, dipeptidase-2.

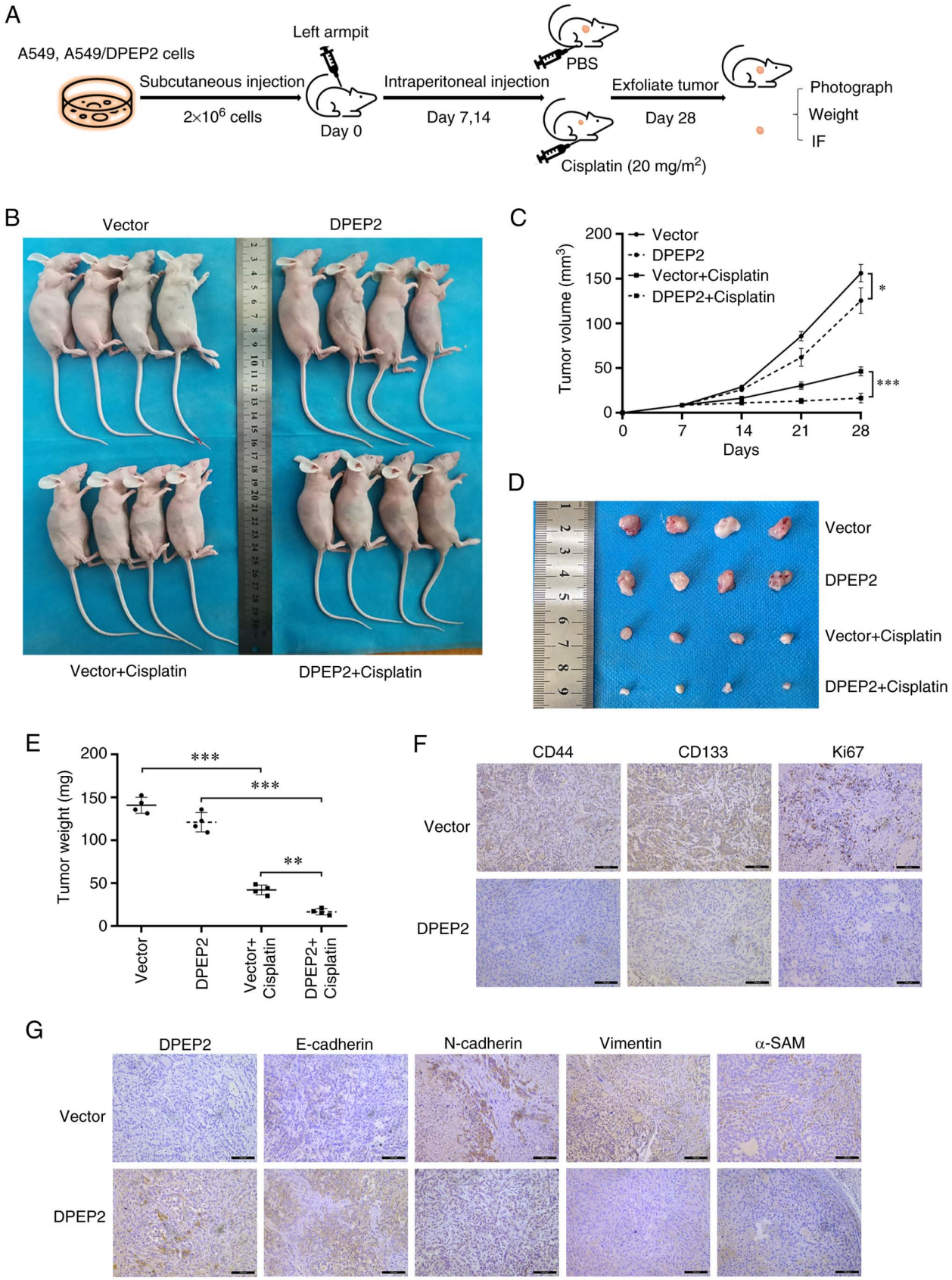

Figure 5. DPEP2 enhances the sensitivity of lung adenocarcinoma cells to cisplatin *in vivo*. (A) Flow chart of the *in vivo* experiment with nude mice. (B and C) Nude mice were subcutaneously injected with a vector or DPEP2-overexpressing A549 stable strain. On days 7 and 14, mice were injected with PBS or cisplatin (20 mg/m^2). Every 7 days, the tumor volume was measured with calipers. Tumor volume on day 28 was assessed using a two-tailed Student's t-test (vector vs. DPEP2; and vector + cisplatin vs. DPEP2 + cisplatin). *P<0.05 and ***P<0.001. (D and E) On day 28, tumors were excised and weighed. Representative tumors isolated from nude mice and average tumor weights. **P<0.01 and ***P<0.001, one-way ANOVA with post hoc Dunnett's t-test. (F and G) Immunohistochemical staining of DPEP2, epithelial-mesenchymal transition-associated genes (E-cadherin, N-cadherin, vimentin, and α-SMA), stem cell biomarkers (CD44 and CD133), and the proliferation marker Ki67 in tumors of mice injected with vector or DPEP2-overexpressing cells (scale bar, 100 μm). DPEP2, dipeptidase-2.

experiments, IHC evaluation showed that DPEP2 overexpression markedly decreased EMT marker genes (N-cadherin, vimentin, and α-SMA), stem cell biomarkers (CD44 and CD133), and the proliferation marker Ki67, and increased E-cadherin expression in tumor tissues (Fig. 5F and G).

Discussion

Lung cancer is the leading cause of cancer-related deaths worldwide, and LUAD is the most prevalent subtype (1). Advances in LUAD treatment have identified the histone chaperone ASF1A (36), methyltransferase-like 7B (37), and the long non-coding RNA HIF1A-AS2 (38) as targets to disrupt drug resistance. Despite these advances, both metastasis and drug resistance remain key characteristics of LUAD, resulting in high rates of recurrence and mortality (39,40).

In the present study, differential expression analysis of RNA sequencing data was performed and it was revealed that *DPEP2* was included in the genes that were substantially downregulated during LUAD progression. Previous studies have revealed that DPEP2 plays a role in immune cells, regulating inflammation caused by macrophages (20) and can be used as an immune indicator to identify lung adenocarcinoma (22). In addition, similar studies have identified DPEP1 as a therapeutic target for neutrophil-driven pulmonary inflammatory diseases (41) and DPEP3 may be associated with rat rheumatoid arthritis (42). Although DPEP2 has been studied in the metabolic and immune indexes of LUAD, the specific mechanism of its effect on the progression of LUAD remains unclear. Therefore, the expression and clinical significance of DPEP2 in LUAD was investigated to determine its functions and regulatory pathways.

In recent years, an increasing number of cancer researchers have used data to reveal disease-related genes and their potential functions via bioinformatics analysis (43,44). Based on information from several major databases such as GEO,TCGA and TIMER2.0 databases, both DPEP2 expression and the mutation rate were low in LUAD, with similar results *in vitro*. In addition to indicators such as age and sex, cancer grade and stage play a significant role in influencing patient prognosis. The higher the tumor grade and stage, the higher the likelihood of metastasis and the worse the prognosis (45). In the present study, it was demonstrated that low DPEP2 expression was associated with poor clinicopathological features and poor OS in patients with LUAD and that DPEP2 is an independent prognostic factor, which was consistent with a previous study (21). In addition, the area under the ROC curve of DPEP2 expression data was 0.976, which is close to the maximum value of 1, suggesting good diagnostic value. These findings indicated that DPEP2 may serve as a prognostic biomarker in LUAD. However, the mechanism of action of DPEP2 on LUAD remains unclear.

To better understand the role of DPEP2 in LUAD, functional and mechanistic experiments were conducted. It was revealed that DPEP2 overexpression inhibited cell migration and invasion. Previous similar studies have also demonstrated that the expression of DPEP1 in colon cancer and pancreatic ductal adenocarcinoma cells influences the aggressiveness of cancer cells (27,46,47). Studies have shown that cell migration and invasion are a feature of EMT. EMT is a reversible cellular program that transforms epithelial cells into mesenchymal cell states (8) and is a key event in metastasis, invasion, and diffusion to distant organs (48). In addition, EMT is highly associated with tumor prognosis. For example, TFAP2A increased LUAD metastasis by positively regulating the EMT process (49). FAM83A may play a key role in promoting LUAD progression by influencing EMT (50). Similarly, the results of the present study indicated that DPEP2 can affect the progression of LUAD by inhibiting EMT, thus inhibiting the migration and invasion of LUAD cells *in vitro*.

Previous studies have revealed a strong correlation between EMT and cancer stem cell properties (51). EMT can enable cancer stem cells to migrate to other organs and permit site colonization (52). In addition, cancer stem cells have sufficient multidirectional differentiation ability to undergo EMT (53). In lung cancer, a variety of markers including CD44, CD133, CD24, ALCAM, OCT4, NANOG, and LGR5 are known to be related to cell stemness, with CD44 and CD133 being more important (54-57). Previous studies have demonstrated that EMT can affect the process of tumor formation through cell stemness (8,35,58), thus the effect of DPEP2 on the stem cell marker CD44/CD133 was detected through western blotting and IF experiments, as a superficial verification, without in-depth investigation of its mechanism. Therefore, the expression of CD44/CD133 was not detected by FACS analysis. The lack of FACS analysis of the stemness markers is a limitation of this study. In the present study, it was determined that DPEP2 overexpression decreased CD44 and CD133 protein levels. Moreover, sphere formation indicated that DPEP2 overexpression inhibited cell stemness. These results indicated that DPEP2 may inhibit EMT in LUAD cells by regulating tumor stemness.

Furthermore, the role of DPEP2 in chemotherapy resistance was investigated *in vitro* and *in vivo*. Cisplatin is a first-line chemotherapy drug for lung cancer (59). Colony formation and flow cytometry revealed that DPEP2 overexpression increased the sensitivity of A549 and H1650 cells to cisplatin. Similar studies on cisplatin resistance also revealed, for example, DPEP1 inhibited invasiveness and enhanced the chemical sensitivity of pancreatic ductal adenocarcinoma cells (28), CCT3 promoted cisplatin resistance in LUAD cells (60), and TRIM44 overexpression conferred cisplatin resistance in LUAD (61). Therefore, a nude mouse subcutaneous tumor model was successfully constructed and it was demonstrated that tumor nodules formed by DPEP2-overexpressing cells decreased in size and weight, indicating increased sensitivity to cisplatin. Moreover, IHC demonstrated that DPEP2 overexpression could inhibit the expression of EMT- and stem cell transformation-related markers. These results indicated that DPEP2 enhanced the efficacy of cisplatin and reduced tumor progression by inhibiting EMT.

However, despite the analytical exploration of DPEP2 and cross-validation using databases and *in vitro* and *in vivo* experiments, there are some limitations to this study. First, the number of cell lines and animal models used were limited, which may in turn limit the clinical applicability of the results. Thus, the results need to be validated in larger studies. Second, the mechanism by which DPEP2 affects the stemness to regulate the progression of LUAD has not been thoroughly discussed, and will be further investigated through the search and identification of functional targets in the future. These issues are worthy of further investigation.

In conclusion, the present study revealed a novel association between DPEP2 and LUAD progression, as low DPEP2 expression was positively associated with poor prognosis and poor OS in patients with LUAD. DPEP2 inhibited migration, metastasis, and EMT by regulating the transformation of cancer stem cells, thereby increasing the sensitivity of LUAD to cisplatin. These results indicated that DPEP2 may affect patient survival and serve as a prognostic biomarker in LUAD. The findings of the present study suggest that DPEP2 is a potential therapeutic target for future therapeutic research in LUAD.

Acknowledgements

Not applicable.

Funding

The present study was funded by the National Natural Science Foundation of China (grant nos. 81972977 and 81802955), the Foundation of Health Commission of Chengdu (grant no. 2021001), the Foundation of Chengdu Science and Technology Bureau (grant no. 2021-YF05-00291-SN), the Foundation of The First Affiliated Hospital of Chengdu Medical College (grant no. CYFY2021LNZD01), the Foundation of Chengdu Medical College and Chengdu Xindu District People's Hospital Joint Research (grant no. 2021LHZD-07), and the Foundation of Graduate Innovation and Chengdu Medical College (grant no. YCX2022-03-03).

Availability of data and materials

The datasets used and/or analyzed during the current study are available from the corresponding author on reasonable request.

Authors' contributions

YW, TZ, HD and MY collected data. YW and TZ wrote, reviewed, and edited the manuscript. GX, TL and SD revised the study critically for important intellectual content. WY and SH confirm the authenticity of all the raw data. DW and YX directed the project and wrote, reviewed, and edited the manuscript. All authors contributed to manuscript composition, and all authors read and approved the final manuscript.

Ethics approval and consent to participate

All xenograft experiments were performed in accordance with the guidelines of the Laboratory Animal Ethics Committee of Chengdu Medical College (Chengdu, China). All experimental protocols were approved by the Experimental Animal Ethics Committee of Chengdu Medical College (approval no. 2021-096).

Patient consent for publication

Not applicable.

Competing interests

The authors declare that they have no competing interests.

References

1. Sung H, Ferlay J, Siegel RL, Laversanne M, Soerjomataram I, Jemal A and Bray F: Global Cancer Statistics 2020: GLOBOCAN Estimates of Incidence and Mortality Worldwide for 36 Cancers in 185 Countries. CA Cancer J Clin 71: 209-249, 2021.
2. Gong L, Hu Y, He D, Zhu Y, Xiang L, Xiao M, Bao Y, Liu X, Zeng Q, Liu J, *et al*: Ubiquitin ligase CHAF1B induces cisplatin resistance in lung adenocarcinoma by promoting NCOR2 degradation. Cancer Cell Int 20: 194, 2020.
3. Esai Selvan M, Zauderer MG, Rudin CM, Jones S, Mukherjee S, Offit K, Onel K, Rennert G, Velculescu VE, Lipkin SM, *et al*: Inherited rare, deleterious variants in ATM increase lung adenocarcinoma risk. J Thorac Oncol 15: 1871-1879, 2020.
4. Li Y, Zhang H, Fan L, Mou J, Yin Y, Peng C, Chen Y, Lu H, Zhao L, Tao Z, *et al:* MiR-629-5p promotes the invasion of lung adenocarcinoma via increasing both tumor cell invasion and endothelial cell permeability. Oncogene 39: 3473-3488, 2020.
5. Rose MC, Kostyanovskaya E and Huang RS: Pharmacogenomics of cisplatin sensitivity in non-small cell lung cancer. Genomics Proteomics Bioinformatics 12: 198-209, 2014.
6. Bakir B, Chiarella AM, Pitarresi JR and Rustgi AK: EMT, MET, plasticity, and tumor metastasis. Trends Cell Biol 30: 764-776, 2020.
7. Piera-Velazquez S and Jimenez SA: Endothelial to mesenchymal transition: Role in physiology and in the pathogenesis of human diseases. Physiol Rev 99: 1281-1324, 2019.
8. Dongre A and Weinberg RA: New insights into the mechanisms of epithelial-mesenchymal transition and implications for cancer. Nat Rev Mol Cell Biol 20: 69-84, 2019.
9. Gao ZW, Liu C, Yang L, Chen HC, Yang LF, Zhang HZ and Dong K: CD73 severed as a potential prognostic marker and promote lung cancer cells migration via enhancing EMT progression. Front Genet 12: 728200, 2021.
10. Yu TT, Zhang T, Su F, Li YL, Shan L, Hou XM and Wang RZ: ELK1 Promotes epithelial-mesenchymal transition and the progression of lung adenocarcinoma by upregulating B7-H3. Oxid Med Cell Longev 2021: 2805576, 2021.
11. Liu Z, Liu J, Li Y, Wang H, Liang Z, Deng X, Fu Q, Fang W and Xu P: VPS33B suppresses lung adenocarcinoma metastasis and chemoresistance to cisplatin. Genes Dis 8: 307-319, 2021.
12. Chua KN, Poon KL, Lim J, Sim WJ, Huang RY and Thiery JP: Target cell movement in tumor and cardiovascular diseases based on the epithelial-mesenchymal transition concept. Adv Drug Deliv Rev 63: 558-567, 2011.
13. Chen T, You Y, Jiang H and Wang ZZ: Epithelial-mesenchymal transition (EMT): A biological process in the development, stem cell differentiation, and tumorigenesis. J Cell Physiol 232: 3261-3272, 2017.
14. Habib GM, Shi ZZ, Cuevas AA and Lieberman MW: Identification of two additional members of the membrane-bound dipeptidase family. FASEB J 17: 1313-1315, 2003.
15. Kozak EM and Tate SS: Glutathione-degrading enzymes of microvillus membranes. J Biol Chem 257: 6322-6327, 1982.
16. Habib GM, Shi ZZ, Cuevas AA, Guo Q, Matzuk MM and Lieberman MW: Leukotriene D4 and cystinyl-bis-glycine metabolism in membrane-bound dipeptidase-deficient mice. Proc Natl Acad Sci USA 95: 4859-63, 1998.
17. Park SY, Lee SJ, Cho HJ, Kim TW, Kim JT, Kim JW, Lee CH, Kim BY, Yeom YI, Lim JS, *et al*: Dehydropeptidase 1 promotes metastasis through regulation of E-cadherin expression in colon cancer. Oncotarget 7: 9501-9512, 2016.
18. Hayashi K, Longenecker KL, Koenig P, Prashar A, Hampl J, Stoll V and Vivona S: Structure of human DPEP3 in complex with the SC-003 antibody Fab fragment reveals basis for lack of dipeptidase activity. J Struct Biol 211: 107512, 2020.
19. von Mässenhausen A, Zamora Gonzalez N, Maremonti F, Belavgeni A, Tonnus W, Meyer C, Beer K, Hannani MT, Lau A, Peitzsch M, *et al*: Dexamethasone sensitizes to ferroptosis by glucocorticoid receptor-induced dipeptidase-1 expression and glutathione depletion. Sci Adv 8: eabl8920, 2022.
20. Yang X, Yue Y and Xiong S: Dpep2 emerging as a modulator of macrophage inflammation confers protection against CVB3-induced viral myocarditis. Front Cell Infect Microbiol 9: 57, 2019.
21. Huang G, Zhang J, Gong L, Wang X, Zhang B and Liu D: Characterization of the fatty acid metabolism-related genes in lung adenocarcinoma to guide clinical therapy. BMC Pulm Med 22: 486, 2022.

22. Han T, Liu Y, Wu J, Bai Y, Zhou J, Hu C, Zhang W, Guo J, Wang Q and Hu D: An immune indicator based on BTK and DPEP2 identifies hot and cold tumors and clinical treatment outcomes in lung adenocarcinoma. Sci Rep 13: 5153, 2023.
23. Hamilton E, O'Malley DM, O'Cearbhaill R, Cristea M, Fleming GF, Tariq B, Fong A, French D, Rossi M, Brickman D and Moore K: Tamrintamab pamozirine (SC-003) in patients with platinum-resistant/refractory ovarian cancer: Findings of a phase 1 study. Gynecol Oncol 158: 640-645, 2020.
24. Yoshitake H, Yanagida M, Maruyama M, Takamori K, Hasegawa A and Araki Y: Molecular characterization and expression of dipeptidase 3, a testis-specific membrane-bound dipeptidase: Complex formation with TEX101, a germ-cell-specific antigen in the mouse testis. J Reprod Immunol 90: 202-213, 2011.
25. Schiza C, Korbakis D, Panteleli E, Jarvi K, Drabovich AP and Diamandis EP: Discovery of a human testis-specific protein complex TEX101-DPEP3 and selection of its disrupting antibodies. Mol Cell Proteomics 17: 2480-2495, 2018.
26. Hao JJ, Zhi X, Wang Y, Zhang Z, Hao Z, Ye R, Tang Z, Qian F, Wang Q and Zhu J: Comprehensive proteomic characterization of the human colorectal carcinoma reveals signature proteins and perturbed pathways. Sci Rep 7: 42436, 2017.
27. Wu YF, Wang CY, Tang WC, Lee YC, Ta HDK, Lin LC, Pan SR, Ni YC, Anuraga G and Lee KH: Expression profile and prognostic value of Wnt signaling pathway molecules in colorectal cancer. Biomedicines 9: 1331, 2021.
28. Zhang G, Schetter A, He P, Funamizu N, Gaedcke J, Ghadimi BM, Ried T, Hassan R, Yfantis HG, Lee DH, *et al*: DPEP1 inhibits tumor cell invasiveness, enhances chemosensitivity and predicts clinical outcome in pancreatic ductal adenocarcinoma. PLoS One 7: e31507, 2012.
29. Cui X, Liu X, Han Q, Zhu J, Li J, Ren Z, Liu L, Luo Y, Wang Z, Zhang D, *et al*: DPEP1 is a direct target of miR-193a-5p and promotes hepatoblastoma progression by PI3K/Akt/mTOR pathway. Cell Death Dis 10: 701, 2019.
30. Zhang W, Chen T, Liu J, Yu S, Liu L, Zheng M, Liu Y, Zhang H, Bian T and Zhao X: RAB11FIP1: An indicator for tumor immune microenvironment and prognosis of lung adenocarcinoma from a comprehensive analysis of bioinformatics. Front Genet 12: 757169, 2021.
31. Okayama H, Kohno T, Ishii Y, Shimada Y, Shiraishi K, Iwakawa R, Furuta K, Tsuta K, Shibata T, Yamamoto S, *et al*: Identification of genes upregulated in ALK-positive and EGFR/KRAS/ALK-negative lung adenocarcinomas. Cancer Res 72: 100-111, 2012.
32. Yamauchi M, Yamaguchi R, Nakata A, Kohno T, Nagasaki M, Shimamura T, Imoto S, Saito A, Ueno K, Hatanaka Y, *et al*: Epidermal growth factor receptor tyrosine kinase defines critical prognostic genes of stage I lung adenocarcinoma. PLoS One 7: e43923, 2012.
33. Livak KJ and Schmittgen TD: Analysis of relative gene expression data using real-time quantitative PCR and the 2(-Delta Delta C(T)) method. Methods 25: 402-408, 2001.
34. Zhu G, Cheng Z, Huang Y, Zheng W, Yang S, Lin C and Ye J: MyD88 mediates colorectal cancer cell proliferation, migration and invasion via NF-κB/AP-1 signaling pathway. Int J Mol Med 45: 131-140, 2020.
35. Wu DM, Zhang T, Liu YB, Deng SH, Han R, Liu T, Li J and Xu Y: The PAX6-ZEB2 axis promotes metastasis and cisplatin resistance in non-small cell lung cancer through PI3K/AKT signaling. Cell Death Dis 10: 349, 2019.
36. Li F, Huang Q, Luster TA, Hu H, Zhang H, Ng WL, Khodadadi-Jamayran A, Wang W, Chen T, Deng J, *et al*: In Vivo Epigenetic CRISPR screen identifies Asf1a as an immunotherapeutic target in Kras-Mutant lung adenocarcinoma. Cancer Discov 10: 270-287, 2020.
37. Song H, Liu D, Wang L, Liu K, Chen C, Wang L, Ren Y, Ju B, Zhong F, Jiang X, *et al*: Methyltransferase like 7B is a potential therapeutic target for reversing EGFR-TKIs resistance in lung adenocarcinoma. Mol Cancer 21: 43, 2022.
38. Si J, Ma Y, Lv C, Hong Y, Tan H and Yang Y: HIF1A-AS2 induces osimertinib resistance in lung adenocarcinoma patients by regulating the miR-146b-5p/IL-6/STAT3 axis. Mol Ther Nucleic Acids 26: 613-624, 2021.
39. Chaffer CL and Weinberg RA: A perspective on cancer cell metastasis. Science 331: 1559-1564, 2011.
40. Chen J, Liu X, Xu Y, Zhang K, Huang J, Pan B, Chen D, Cui S, Song H, Wang R, *et al*: TFAP2C-Activated MALAT1 modulates the chemoresistance of docetaxel-resistant lung adenocarcinoma cells. Mol Ther Nucleic Acids 14: 567-582, 2019.
41. Choudhury SR, Babes L, Rahn JJ, Ahn BY, Goring KR, King JC, Lau A, Petri B, Hao X, Chojnacki AK, *et al*: Dipeptidase-1 is an adhesion receptor for neutrophil recruitment in lungs and liver. Cell 178: 1205-1221.e17, 2019.
42. Lai W, Wang C, Lai R, Peng X and Luo J: Lycium barbarum polysaccharide modulates gut microbiota to alleviate rheumatoid arthritis in a rat model. NPJ Sci Food 6: 34, 2022.
43. Song X, Du R, Gui H, Zhou M, Zhong W, Mao C and Ma J: Identification of potential hub genes related to the progression and prognosis of hepatocellular carcinoma through integrated bioinformatics analysis. Oncol Rep 43: 133-146, 2020.
44. Chen J, Xu D, Wang T, Yang Z, Yang Y, He K and Zhao L: HMGB1 promotes the development of castration resistant prostate cancer by regulating androgen receptor activation. Oncol Rep 48: 197, 2022.
45. Yamanashi K, Menju T, Hamaji M, Tanaka S, Yutaka Y, Yamada Y, Nakajima D, Ohsumi A, Aoyama A, Sato T, *et al*: Prognostic factors related to postoperative survival in the newly classified clinical T4 lung cancer. Eur J Cardiothorac Surg 57: 754-761, 2020.
46. Toiyama Y, Inoue Y, Yasuda H, Saigusa S, Yokoe T, Okugawa Y, Tanaka K, Miki C and Kusunoki M: DPEP1, expressed in the early stages of colon carcinogenesis, affects cancer cell invasiveness. J Gastroenterol 46: 153-163, 2011.
47. Zeng C, Qi G, Shen Y, Li W, Zhu Q, Yang C, Deng J, Lu W, Liu Q and Jin J: DPEP1 promotes drug resistance in colon cancer cells by forming a positive feedback loop with ASCL2. Cancer Med 12: 412-424, 2023.
48. Mittal V: Epithelial mesenchymal transition in tumor metastasis. Annu Rev Pathol 13: 395-412, 2018.
49. Xiong Y, Feng Y, Zhao J, Lei J, Qiao T, Zhou Y, Lu Q, Jiang T, Jia L and Han Y: TFAP2A potentiates lung adenocarcinoma metastasis by a novel miR-16 family/TFAP2A/PSG9/TGF-β signaling pathway. Cell Death Dis 12: 352, 2021.
50. Liu X, Fu M, Xia D, Ji Z, Hu N, Leng Z, Xie W, Fang Y and Zhang J: Overexpression of FAM83A is associated with poor prognosis of lung adenocarcinoma. J Oncol 2022: 8767333, 2022.
51. Thiery JP, Acloque H, Huang RY and Nieto MA: Epithelial-mesenchymal transitions in development and disease. Cell 139: 871-890, 2009.
52. Kavanagh DP, Robinson J and Kalia N: Mesenchymal stem cell priming: Fine-tuning adhesion and function. Stem Cell Rev Rep 10: 587-599, 2014.
53. McCabe EM and Rasmussen TP: lncRNA involvement in cancer stem cell function and epithelial-mesenchymal transitions. Semin Cancer Biol 75: 38-48, 2021.
54. Leung EL, Fiscus RR, Tung JW, Tin VP, Cheng LC, Sihoe AD, Fink LM, Ma Y and Wong MP: Non-small cell lung cancer cells expressing CD44 are enriched for stem cell-like properties. PLoS One 5: e14062, 2010.
55. Hess DA, Wirthlin L, Craft TP, Herrbrich PE, Hohm SA, Lahey R, Eades WC, Creer MH and Nolta JA: Selection based on CD133 and high aldehyde dehydrogenase activity isolates long-term reconstituting human hematopoietic stem cells. Blood 107: 2162-2169, 2006.
56. Prasetyanti PR and Medema JP: Intra-tumor heterogeneity from a cancer stem cell perspective. Mol Cancer 16: 41, 2017.
57. Jiang P, Li F, Liu Z, Hao S, Gao J and Li S: BTB and CNC homology 1 (Bach1) induces lung cancer stem cell phenotypes by stimulating CD44 expression. Respir Res 22: 320, 2021.
58. Pan G, Liu Y, Shang L, Zhou F and Yang S: EMT-associated microRNAs and their roles in cancer stemness and drug resistance. Cancer Commun (Lond) 41: 199-217, 2021.
59. Konoshenko M, Lansukhay Y, Krasilnikov S, Laktionov P: MicroRNAs as predictors of lung-cancer resistance and sensitivity to cisplatin. Int J Mol Sci 23: 7594, 2022.
60. Danni X, Jiangzheng Z, Huamao S, Yinglian P, Changcheng Y and Yanda L: Chaperonin containing TCP1 subunit 3 (CCT3) promotes cisplatin resistance of lung adenocarcinoma cells through targeting the Janus kinase 2/signal transducers and activators of transcription 3 (JAK2/STAT3) pathway. Bioengineered 12: 7335-7347, 2021.
61. Zhang S, Cao M, Yan S, Liu Y, Fan W, Cui Y, Tian F, Gu R, Cui Y, Zhan Y, *et al*: TRIM44 promotes BRCA1 functions in HR repair to induce Cisplatin Chemoresistance in Lung Adenocarcinoma by Deubiquitinating FLNA. Int J Biol Sci 18: 2962-2979, 2022.